ABFST-model description of $\pi^+ p \to 3\pi^+ 2\pi^- p$ and related processes*

Jan W. Dash†
Argonne National Laboratory, Argonne, Illinois 60439

J. Huskins
Physics Department, Imperial College, London S.W. 7, England

S. T. Jones‡
University of Alabama, University, Alabama 35486

(Received 23 October 1973)

The ABFST (Amati-Bertocchi-Fubini-Stanghellini-Tonin) model modified by a particular off-shell $\pi\pi$-resonance vertex is shown to yield a reasonable description of the reaction $\pi^+ p \to 3\pi^+ 2\pi^- p$ in normalization, energy dependence, and distributions. The off-shell modification is consistent with that required in theoretical calculations of the bare Pomeron at $\hat{\alpha}_0 \sim 0.8$ via the ABFST model. The calculation is also consistent with factorization of the ABFST model in describing certain four-prong cross sections by single pion exchange.

I. INTRODUCTION

The description of exclusive multiparticle reactions remains a basic challenge of hadron physics. While inclusive reactions can demonstrate certain simple patterns describable through unitarity and a generalized Regge phenomenology, detailed dynamical models must sooner or later come to grips with the much more complicated task of describing exclusive distributions. Multiperipheral models seem to hold considerable promise in describing various qualitative aspects of inclusive reactions. It remains to be seen whether a realistic *specific* multiperipheral model can be found. From a theoretical viewpoint, the ABFST (Amati-Bertocchi-Fubini-Stanghellini-Tonin) model[1] is a promising candidate. However, it is known that if the ABFST model is to provide a model for the bulk of the inelastic cross section, the physical $\pi\pi X$ (X=resonance) couplings are insufficiently strong to generate anything near a constant energy dependence.[2] If an enhancing off-shell behavior of the $\pi\pi X$ couplings is included, much more reasonable results are obtained.[3] Part of our exercise here is to show that the same sort of enhanced off-shell $\pi\pi X$ behavior is needed if the ABFST model is to successfully describe the reaction σ_6^+ defined below in Eq. (1). We regard this as providing a partial verification of the consistency of the approach. More convincing arguments would depend on other successful exclusive applications of the model, and additional applications are currently being pursued.

The reaction we have chosen to study is

$$\sigma_6^+ \equiv \sigma(\pi^+ p \to 3\pi^+ 2\pi^- p)\,. \tag{1}$$

We shall be consistent with one-pion exchange calculations of various 4-prong reactions,[4] such as

$$\pi^+ p \to \rho^0 \Delta^{++}\,, \tag{2}$$

$$p\bar{p} \to \Delta^{++}\bar{\Delta}^{--}\,, \tag{3}$$

This is most important, for by also considering σ_6^+ we are checking the factorization property inherent in the model. It is strange but true that the factorization property of the ABFST model has not been thoroughly examined via comparison with exclusive processes having more than 4 prongs. Factorization is a severe constraint. If, for example, conventional $\pi\pi X$ form factors are used, the shapes of the experimental distributions are reasonably reproduced, but the normalization of σ_6^+ is a factor 5–10 too small.[5] Our $\pi\pi X$ form factor $V_{\rm off}(t_{\pi 1}, t_{\pi 2})$ will be chosen such that

(i) when only one pion is off-shell, the value of $V_{\rm off}(m_\pi^2, t_\pi)$ is in substantial agreement with conventional form factors;

(ii) $V_{\rm off}(t', t')$ for $t_{\pi 1} = t_{\pi 2} = t'$ is in rough agreement with the off-shell behavior needed in theoretical calculations assuming that the resonance-ABFST model generates the "bare Pomeron" at $\hat{\alpha}_0 \sim 0.8$;[3,6]

(iii) $V_{\rm off}$ has a form consistent with analyticity requirements.

We shall for simplicity choose the baryon (πp-resonance) vertex as that used by Wolf in fitting the 4-prong data. *This, along with (i), automatically guarantees that the 4-prong cross sections (2) and (3) will be fitted here as well as the one-pion exchange model usually fits them.* Insofar as this description is quite reasonable,[4,7] we need not consider these 4-prong reactions further.

Our form for $V_{\rm off}$ is

$$V_{\rm off}(t_{\pi 1}, t_{\pi 2}) = \left(1 - \frac{\tilde{t}_{\pi 1}}{\lambda} - \frac{\tilde{t}_{\pi 2}}{\lambda} + \frac{\tilde{t}_{\pi 1}\tilde{t}_{\pi 2}}{\xi}\right) e^{b(\tilde{t}_{\pi 1}+\tilde{t}_{\pi 2})} , \tag{4}$$

where $\tilde{t} \equiv t - m_\pi{}^2$.

This function has three parameters: λ, b, and ξ. They are the only free parameters in the model. Two of them (λ, b) are roughly fixed by the requirement (i) ($\lambda \sim 1.2$ GeV^2, $b \sim 0.6$ GeV^2). *Thus, the model used to fit* σ_6^+ *has exactly one free parameter,* and the normalization of σ_6^+ fixes

$$\xi \sim 0.15 \text{ GeV}^4.$$

As we have said, our form for $V_{\rm off}$ is roughly that used in Ref. 3 to generate the bare Pomeron.[8] It should be noted that it is taken for simplicity as independent of the s-channel partial-wave value l_s. Indeed, it is implicitly assumed that the threshold behavior in l_s is damped out rapidly, leaving Eq. (4) as the effective behavior for the relevant ranges of momentum transfer. $V_{\rm off}(t', t')$ is typically much larger than conventional form factors, even though $V_{\rm off}(t', m_\pi{}^2)$ agrees with them.

The ABFST model we use is illustrated in Fig. 1. The production amplitude is written as a multiperipheral chain of off-shell 2-2 amplitudes (see Appendix). We will use experimental πp and $\pi\pi$ phase shifts for the on-shell amplitudes. The off-shell amplitudes are then specified by Eq. (4) for the $\pi\pi \to \pi\pi$ amplitude, while as mentioned above, the off-shell πp elastic amplitude is determined for convenience by a conventional (Benecke-Dürr) form factor.[9] Exotic channels (e.g., $\pi^+\pi^+$) are neglected. We shall examine all crossed graphs required by Bose statistics and keep the most important of these, which is not possible in analytic calculations. We shall see that most of these crossed graphs are negligible, and all of them are of decreasing importance with increasing energy.

We should mention those effects not included in the model. The first is baryon exchange, i.e., the generalized u channel, which manifests itself at large t_{pp} (proton-proton momentum transfer). We feel that this effect is the probable cause for those distributions which do not agree with the model. (Similar sentiments are expressed in Ref. 5.) The second effect is diffraction. In the energy range under consideration these effects are negligible in σ_6^+ due to lack of phase space. The third effect is the possible presence of three-pion resonances. Since there is no reliable way of including them, we leave them out. It is encouraging that for the particular exclusive reaction under investigation, no obvious 3π enhancements are observed in the data. The fourth effect is the possible independent emission of pions along the multiperipheral chain.

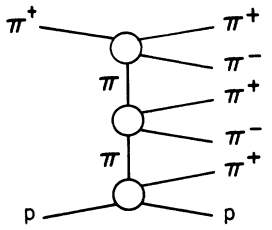

FIG. 1. ABFST diagram for $\pi^+ p \to 3\pi^+ 2\pi^- p$.

Since inclusive charged-neutral particle correlations generally are observed to be so strong, this probably is not an important effect. [It is interesting to speculate that a possible mechanism for including three-pion resonances along with unattached pions may involve a $2\pi \to 4\pi$ kernel with the intermediate state $(3\pi; \pi)$ with the 3π state resonating, but we shall not examine this here.] The fifth effect is the existence of possible absorptive effects of the multiparticle amplitudes, either in the initial two-particle state or the final multiparticle state. These effects are no doubt present and are probably crucial in generating Regge cuts, but as we have no reliable method of estimating their magnitude, we are forced to leave them out. Finally, we have taken the pion as a fixed pole which is wrong, but the additional freedom in Reggeizing it would probably only help things phenomenologically. However, absorption of a Reggeized pion would lead to an effective decrease in its slope α'_π. Owing to the very small subenergies in σ_6^+ this effect would be sizable, making our $\alpha'_\pi = 0$ approximation more reasonable than it might seem *a priori*.

In Sec. II we describe the results of the "fit." The relevant formulas, etc., are given in the Appendix.

II. RESULTS

The reaction σ_6^+ has been measured at 5 GeV/c,[10] 8 GeV/c,[5] and 16 GeV/c.[11] Various experimental analyses have been carried out on the data, including some longitudinal phase-space analysis,[11] which is mainly at 16 GeV/c. This latter analysis is a much better probe into the dynamics than are conventional analyses.

The model calculations were performed using the Monte Carlo event generating program FOWL.[12] 10^5 random events were generated at 16 GeV/c, and the results checked for stability against 5×10^4 additional events. At the lower energies, where phase space is smaller, fewer events were required. Importance sampling was utilized to improve the statistics.

The results for the energy dependence of σ_6^+ are shown in Fig. 2. The agreement with the data is good except at the lower energies. The threshold

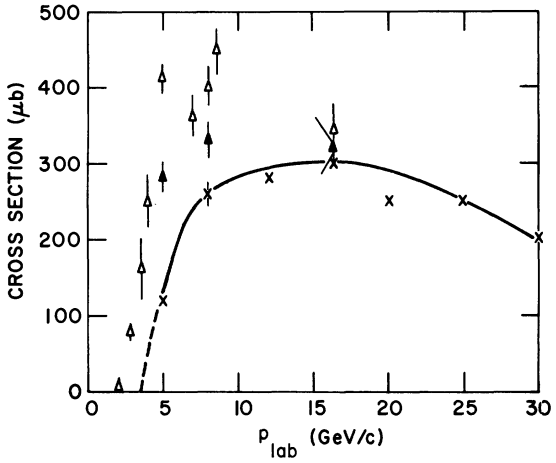

FIG. 2. Total cross section σ_6^+ for the process $\pi^+p \rightarrow 3\pi^+2\pi^-p$. Filled-in triangles denote experimental values with backward protons subtracted. X represents Monte Carlo prediction; a sample statistical error on the theoretical cross section is shown at 8 GeV/c. The curve is a hand fit to the X's.

behavior is clearly not correct. This situation is similar to the pion-exchange description of 4-prong final states, where the OPE (one-pion exchange) contribution becomes more important with increasing energy.[7] However, much of the disagreement is due to the neglect of baryon exchange. When the large proton-proton momentum transfer events, where the proton goes forward, are subtracted from the data to produce the shaded points in Fig. 2, the agreement of the normalization is considerably improved. As our model does not have u-channel effects, this is actually the appropriate comparison. Unfortunately, we cannot make this subtraction in the distributions which have been taken from published experimental papers.

Figures 3 through 6 show comparisons of the model to experimental data at 16 GeV/c. The Monte Carlo curves have been smoothed by hand and have statistical uncertainties of about 10%, except where noted in the captions. They have been normalized to the data in all curves below.

The longitudinal momenta of the pions (Fig. 3) are well fitted, and show characteristic peaking at $p_L = 0$. The π^+'s are slightly more likely to go

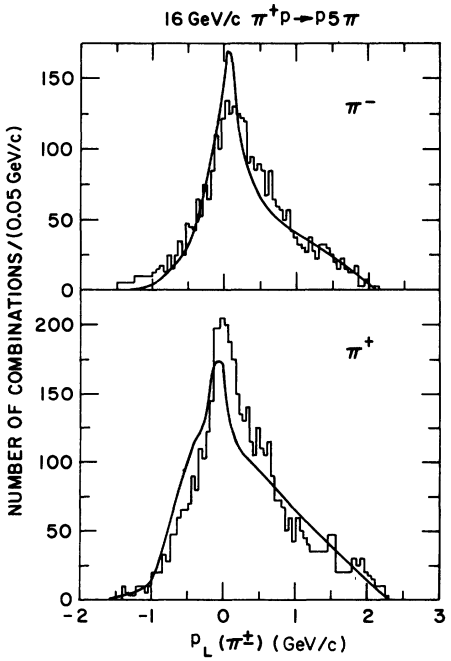

FIG. 3. Longitudinal momentum distributions for $\pi^\pm$ at 16 GeV/c.

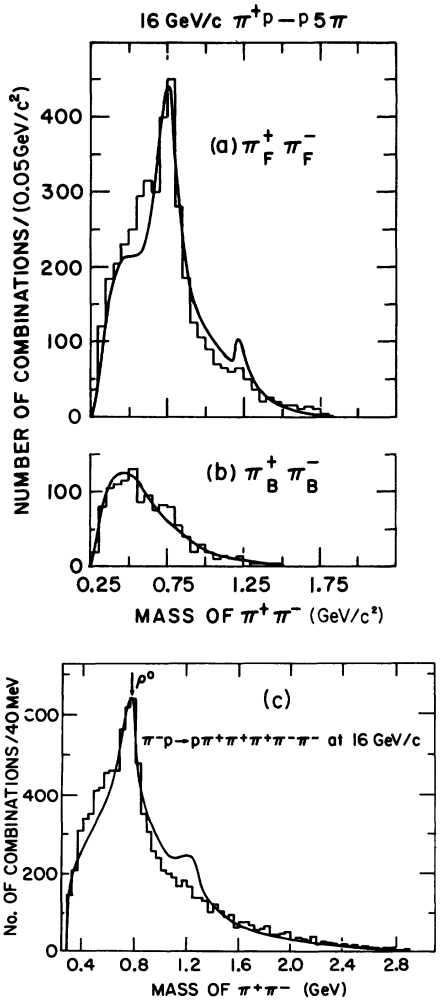

FIG. 4. $\pi^+\pi^-$ invariant mass distributions at 16 GeV/c, for the cases (a) both pions in forward hemisphere; (b) both pions in backward hemisphere; (c) no cuts on the data.

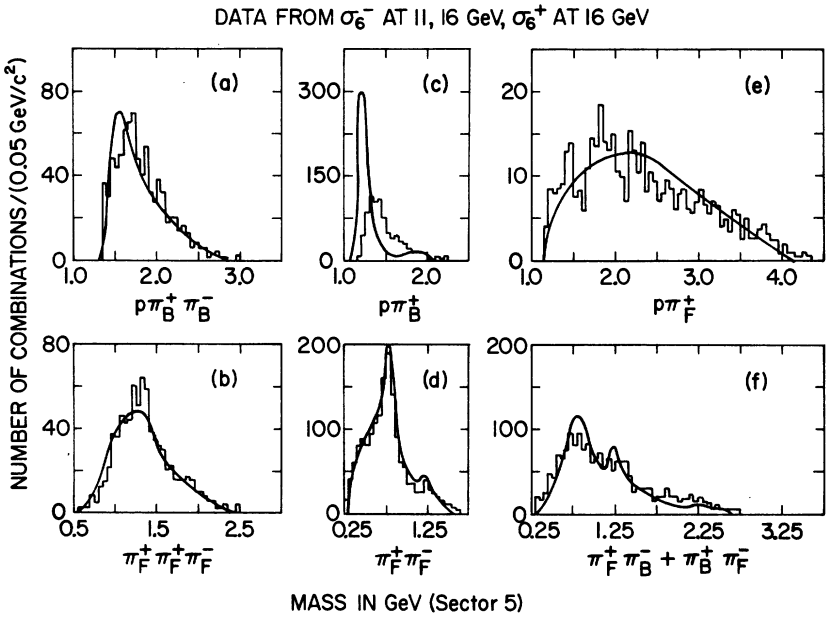

FIG. 5. Invariant mass distributions in LPS sector 5 (see Table I). The experimental histograms are the sum of σ_6^+ at 16 GeV/c, σ_6^- at 11 GeV/c, and σ_6^- at 16 GeV/c. The curve is the model calculation of σ_6^+ at 16 GeV/c. ($\sigma_6^\pm$ are the cross sections for $\pi^\pm p \to 5\pi p$.) Curve 6e has a larger (20%) statistical error than the others. (a) $p\pi_B^+\pi_B^-$; (b) $\pi_F^+\pi_F^+\pi_F^-$; (c) $p\pi_B^+$; (d) $\pi_F^+\pi_F^-$; (e) $p\pi_F^+$; (f) $(\pi_F^+\pi_B^- + \pi_B^+\pi_F^-)$.

forward, as one would naively expect from leading-particle effects.

The over-all $\pi^+\pi^-$ mass distribution at 16 GeV/c is shown in Fig. 4(c). Agreement is good except that the model predicts somewhat too much f_0 production. Figures 4(a) and 4(b) show the $\pi^+\pi^-$ mass distribution in the forward and backward hemispheres. As expected, the model shows no resonance formation between the backward $\pi^+\pi^-$ pair, the π^+ being almost always a decay product of the Δ^{++}. This is in good agreement with the data.

More information is gained from the data when one concentrates on a particular longitudinal phase-space (LPS) sector. Unfortunately, in this LPS analysis, the available published experimental distributions[11] have combined the data from $\sigma_6^-(\pi^- p \to 2\pi^+ 3\pi^- p)$ at 11 and 16 GeV/c, as well as σ_6^+ at 16 GeV/c. (Our model calculation has only been performed for σ_6^+.) We will attempt to point out where the difference between σ_6^- and σ_6^+ is crucial. In Fig. 5 we show the invariant mass distributions in sector 5, defined by and including only those events with the proton and one $\pi^+\pi^-$ pair going backwards in the center-of-mass system. We denote B=backward, F=forward. All distributions are well fitted except for the $p\pi_B^+$ mass, Fig. 5(c). The lack of a strong Δ^{++} peak in the data is probably due to the σ_6^- contribution, where Δ^{++} production is much weaker. (In the framework of the ABFST model, Δ^{++} production in σ_6^- is forbidden since it is accompanied by an off-shell exotic $\pi^-\pi^-$ amplitude, rather than the larger amplitude $\pi^+\pi^-$.) The theoretical distribution in the $(\pi^+\pi^-)$ mass when the two pions are in opposite hemispheres [Fig. 5(f)] shows somewhat more resonance contribution than the data, but is qualitatively correct.

Figure 6 shows the $(\pi^+\pi^-)_F$ mass distribution in LPS sector 8, where all particles other than this forward dipion pair are backward. The 16-GeV/c

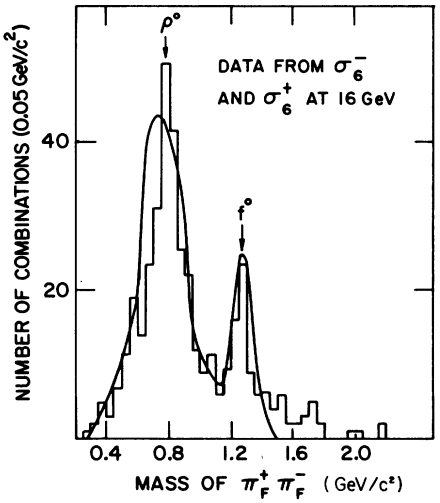

FIG. 6. Invariant mass distribution of forward $\pi^+\pi^-$ pair in sector 8 at 16 GeV/c (see Table I). The experimental histogram is the sum of σ_6^- and σ_6^+.

TABLE I. Normalizations for the various LPS (longitudinal phase space) sectors.

Sector No.	Particles Backward	Particles Forward	Fraction of cross section 5 GeV/c Expt.	5 GeV/c Theor.	8 GeV/c Expt.	8 GeV/c Theor.	16 GeV/c Expt.	16 GeV/c Theor.
1	p	$+++--$	0.01	0.02	0.06	0.02	0.10	0.01
2	$p+$	$++--$	0.10	0.09	0.17	0.17	0.23	0.26
3	$p-$	$+++-$	0.05	0.12	0.06	0.11	0.06	0.02
4	$p++$	$+--$	0.12	0.07	0.12	0.12	0.09	0.17
5	$p+-$	$++-$	0.17	0.30	0.20	0.40	0.21	0.39
6	$p--$	$+++$	0.03	0.13	0.01	0.02	0.01	0.0
7	$p+++$	$--$	0.02	0.01	0.01	0.0	0.0	0.0
8	$p++-$	$+-$	0.10	0.08	0.12	0.08	0.14	0.11
9	$p+--$	$++$	0.04	0.15	0.05	0.06	0.04	0.02
10	$p+++-$	$-$	0.01	0.0	0.0	0.0	0.0	0.0
11	$p++--$	$+$	0.01	0.01	0.02	0.0	0.03	0.0
12-22	mesons	p, mesons	0.33	0.03	0.19	0.005	0.07	0.0

σ_6^- data have been included here also.[11] The ρ and f^0 resonance peaks now stand out distinctly, and the model seems to have about the right amount of each. The lack of a high-mass $\pi\pi$ tail in our $\pi\pi$ amplitude is evident, but not significant at this energy.

Table I shows the normalizations for the various LPS sectors of σ_6^+ at 5, 8, and 16 GeV/c.[11] The statistical errors for both the data for σ_6^+ and the model are substantial. Although most sectors are qualitatively correct, the "u-channel" LPS sector 12–22 has no contribution in the model, as anticipated. The normalization of the fifth sector is the largest one in the model and the data,[11] though the model prediction is too large. Sector 1 is underpopulated, probably due to the fact that in the model the proton is always associated with a π^+. However, this effect is, at most, 10% of σ_6^+. The heavily populated sector 2 is well described by the model. On the whole, the detailed description of the LPS normalizations are qualitatively correct.

Table II shows the results of a simplified LPS analysis, which, although less detailed, is also less subject to statistical fluctuations. It is also more amenable to comparison with the model, as it excludes the baryon-exchange region from the start. Four sectors A – D are defined, as in Ref. 11(b) in the following way. The π^+ and π^- with the smallest values of $|p_L^{\text{c.m.}}|$ are ignored, leaving a pseudo-four-body final state

$$\pi^+ p \to p\pi_F^+\pi_S^+\pi^-(\pi^+\pi^-)_{\text{rejected}},$$

where $p_L(\pi_F^+) > p_L(\pi_S^+)$. The four regions of longitudinal phase space A–D are then [the notation is (backward) (forward)]

A: $(p)_B(\pi_F^+\pi_S^+\pi^-)_F$,

B: $(p\pi^-)_B(\pi_F^+\pi_S^+)_F$,

C: $(p\pi^-\pi_S^+)_B(\pi_F^+)_F$,

D: $(p\pi_S^+)_B(\pi_F^+\pi^-)_F$.

The excluded events are practically all forward proton events, with a few events from sectors 4, 7, 8, and 10 also excluded. The results are consistent with the data at both 8 and 16 GeV/c within the accuracy that we might expect of the model. The normalization of the model is in good agreement with the data.

Figures 7–11 show a comparison of the 8 GeV/c distributions with the data.[5] Most distributions are reasonable. The neglect of u-channel effects shows up in the longitudinal proton momentum distribution [Fig. 7(a)], where the forward-going proton spectrum is not correct. The mass distributions in all cases are well fitted, except for a slight

TABLE II. Results of LPS analysis with baryon exchange excluded.

	Sector	Fraction of cross section σ_{ABCD} A	B	C	D	σ_{ABCD} (mb)
16 GeV/c	Expt.	0.31 ± 0.01	0.09 ± 0.01	0.14 ± 0.01	0.45 ± 0.02	0.32
	Theory [a]	0.33 ± 0.03	0.07 ± 0.01	0.08 ± 0.01	0.52 ± 0.03	0.28
8 GeV/c	Expt.	0.26 ± 0.03	0.12 ± 0.02	0.14 ± 0.02	0.47 ± 0.04	0.31
	Theory [a]	0.30 ± 0.08	0.19 ± 0.03	0.07 ± 0.01	0.44 ± 0.07	0.29

[a] Theoretical errors estimated.

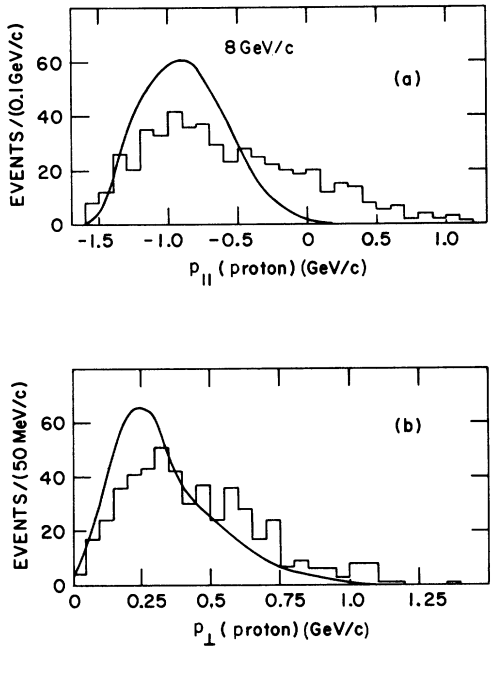

FIG. 7. (a) Longitudinal momentum distribution for proton at 8 GeV/c. (b) Transverse momentum distribution of proton at 8 GeV/c.

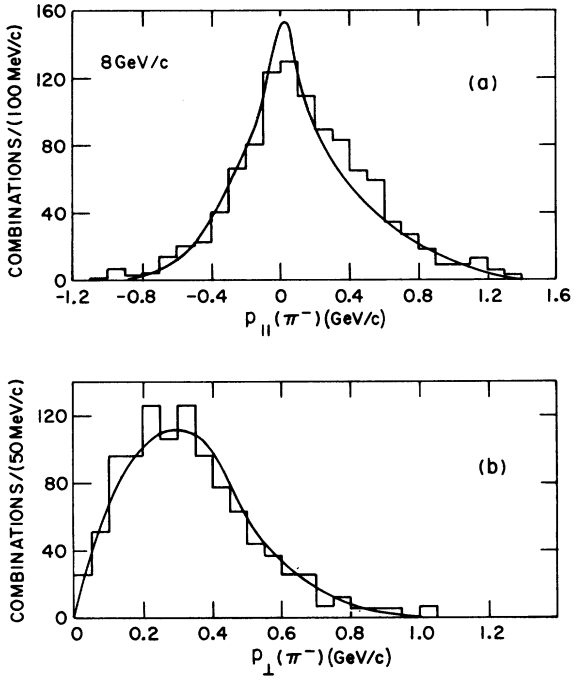

FIG. 9. (a) π^- longitudinal momentum distribution at 8 GeV/c. (b) π^- transverse momentum distribution at 8 GeV/c.

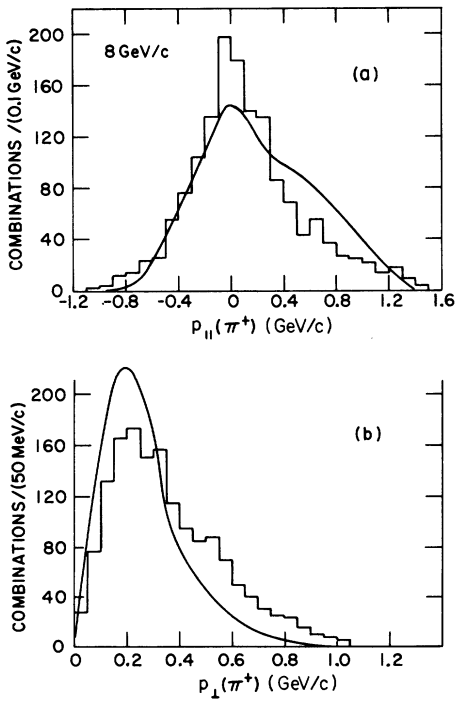

FIG. 8. (a) π^+ longitudinal momentum distribution at 8 GeV/c. (b) π^+ transverse momentum distribution at 8 GeV/c.

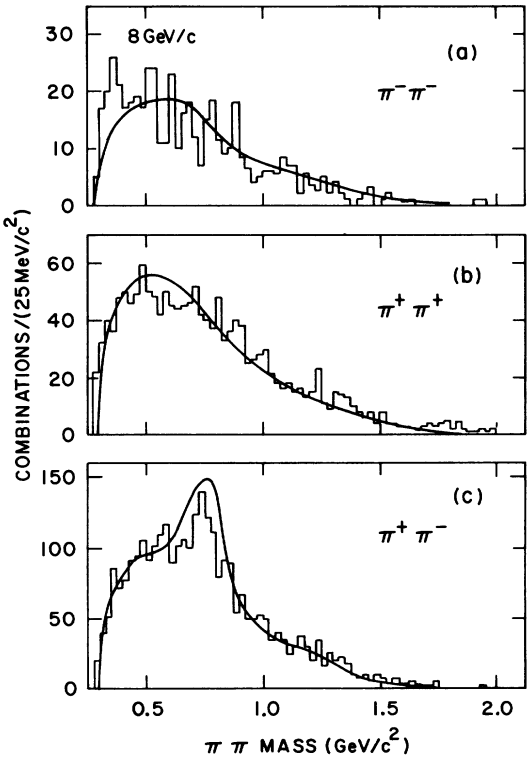

FIG. 10. $\pi\pi$ invariant mass distributions at 8 GeV/c. (a) $\pi^-\pi^-$; (b) $\pi^+\pi^+$; (c) $\pi^+\pi^-$.

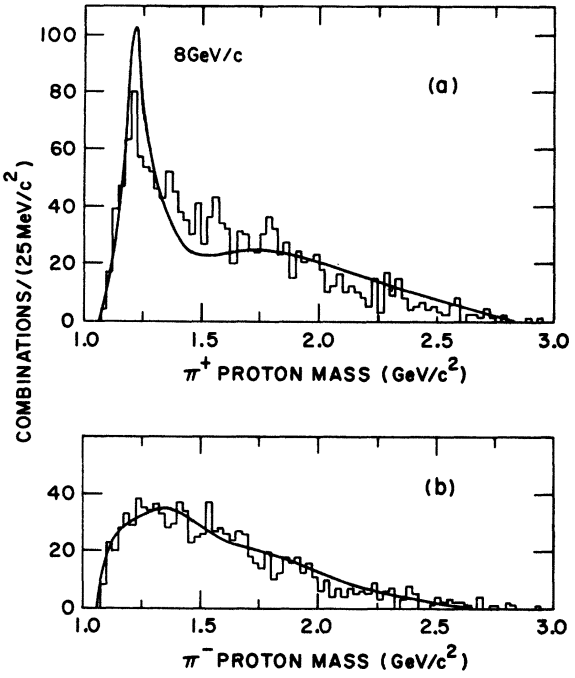

FIG. 11. πp invariant mass distributions at 8 GeV/c. (a) $\pi^+ p$; (b) $\pi^- p$.

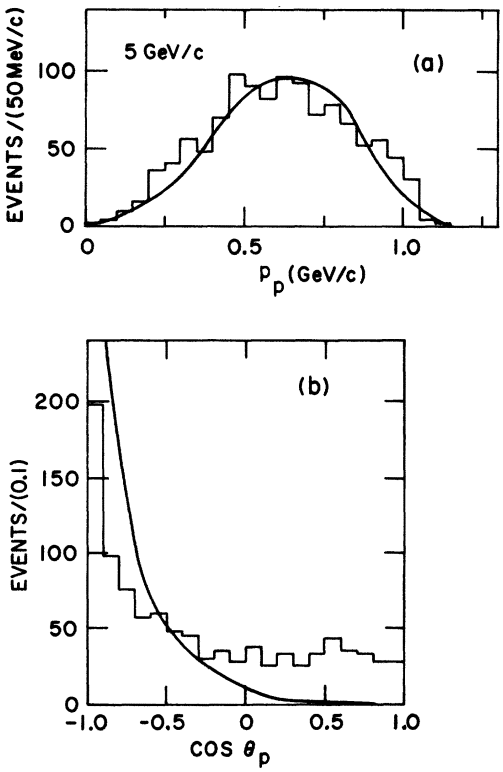

FIG. 12. (a) Magnitude of proton momentum at 5 GeV/c. (b) Cosine of proton scattering angle at 5 GeV/c.

excess of Δ^{++} production [Fig. 11)a)]. This excess is probably also responsible for the excess of small transverse momenta of the proton and π^+'s.

At 5 GeV/c,[10] all distributions (Figs. 12–15) are reasonably described in shape, with the exception again of the proton peripherality [shown in terms of the cosine of the proton scattering angle in Fig. 12(b)]. Figure 13 shows the cosine of the π-π opening angles defined as

$$\cos\theta_{\pi_1\pi_2} = \frac{\vec{p}_1 \cdot \vec{p}_2}{|\vec{p}_1||\vec{p}_2|} \text{ (over-all center-of-mass system)}.$$

The model provides at least a qualitative fit. The slight disagreements are probably due to a somewhat stronger ρ^0 production in the model than in the data. Other than the latter, the mass distributions (Figs. 14 and 15) are very well described.

Summarizing, the fits to the distributions are reasonable. Disagreements exist mainly in distributions associated with the baryon vertex, and can probably be ascribed either to the neglect of baryon exchange or possible inaccuracy of the baryon vertex (which we have not varied from Wolf's parametrization). The π distributions are all reasonable, indicating that our $\pi\pi$ off-shell vertex V_{off} is consistent with the data.

It is of great interest to investigate the extent of peripherality in the model in more detail.

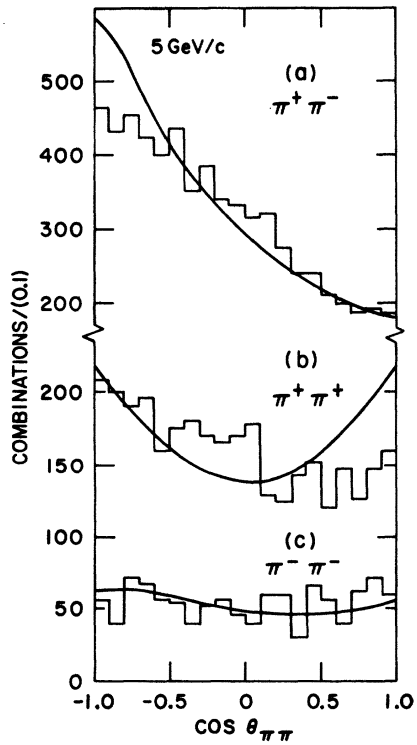

FIG. 13. Cosine of $\pi\pi$ opening angles (defined in text) at 5 GeV/c. (a) $\pi^+\pi^-$; (b) $\pi^+\pi^+$, (c) $\pi^-\pi^-$.

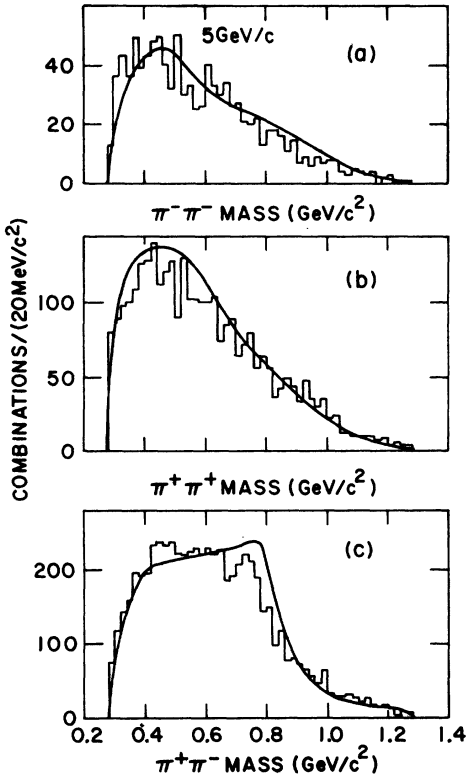

FIG. 14. $\pi\pi$ invariant masses at 5 GeV/c. (a) $\pi^-\pi^-$; (b) $\pi^+\pi^+$; (c) $\pi^+\pi^-$.

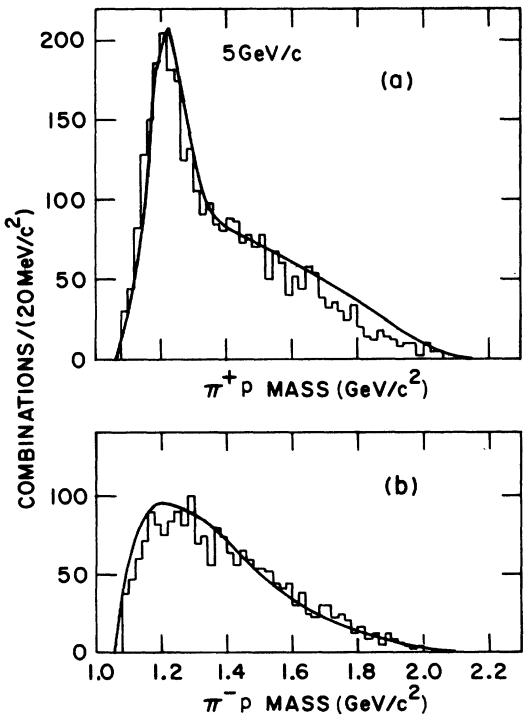

FIG. 15. πp invariant masses at 5 GeV/c. (a) π^+p; (b) π^-p.

Figure 16 shows the momentum transfer distributions t_i of the direct graph at 16 GeV/c. It is seen that the model is highly peripheral, even with the off-shell vertex enhancing large momentum transfers. The average t_i value is around 0.5 GeV^2, and clear t_{min} effects are seen.

Finally, we consider the relative importance of crossed graphs. Figure 17 shows the twelve possible configurations. The first four of these account for approximately 86%, 93%, and 97% of the model for σ_6^+ at 5, 8, and 16 GeV/c, respectively. The direct graph (No. 1) is responsible for 40%, 55%, and 70% of the calculated σ_6^+ at these energies. Thus, most of the graphs are negligible, and the direct graph is the largest contributor. This indicates the extent to which conventional multiperipheral calculations neglecting crossed graphs are valid; it is seen that an error of about a factor of 2 is made by neglecting crossed graphs. It is possible that this could be approximately accounted for in theoretical multiperipheral calculations of σ_{tot} by increasing the average $\pi\pi$ resonance coupling G somewhat. Since $\sigma_6^+ \sim G^4$, we would have to increase G^2 by about $\sqrt{2}$ to accomplish this. An increase of about this magnitude is needed in multi-

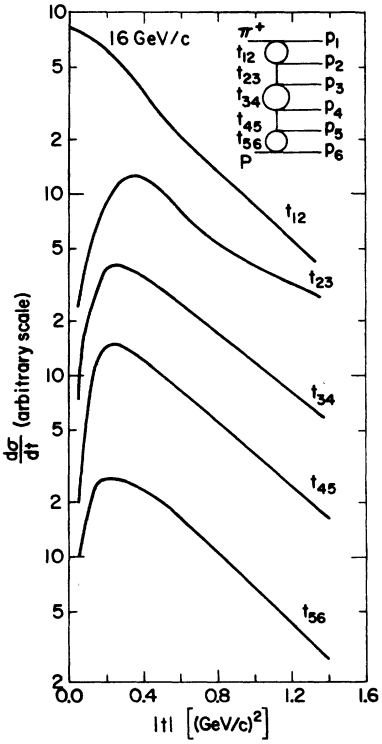

FIG. 16. Invariant momentum transfer distributions at 16 GeV/c. We plot the t_i for the direct graph with the correct total weight. $t_{i(i+1)} = q_i^2$, where q_i = four-momentum of the ith momentum transfer starting from the incident π^+ ($q_i = q_{in} - \sum_{j=1}^{i} p_i$).

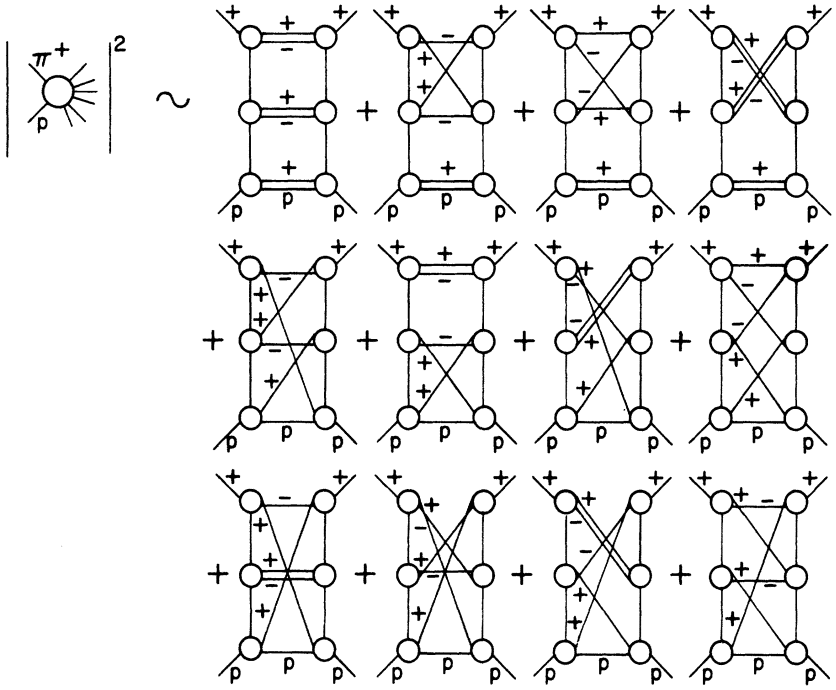

FIG. 17. The 12 graphs contributing to the cross section σ_6^+.

peripheral calculations in addition to V_{off} effects if the bare Pomeron is to have an intercept $\hat{\alpha}_0 \sim 0.8$.[3]

ACKNOWLEDGMENTS

J. W. D. wishes to thank Imperial College, where this work was begun, and the University of Washington, where it was completed, for their hospitality. J. H. thanks the Science Research Council for support, and S. T. J. thanks Argonne National Laboratory for its hospitality and the Argonne Center for Educational Affairs for financial support.

APPENDIX

In this Appendix we present the formalism used in the text. The cross section for the process $\pi^+ p \to 3\pi^+ 2\pi^- p$ is

$$\sigma_6^+(s) = \frac{(2\pi)^{-14}}{3!2!2\lambda^{1/2}(s, m_N^2, m_\pi^2)} \times \int \prod_{i=1}^{6} \frac{d^3p_i}{2E_i} \delta^4\left(p_{\text{in}} + q_{\text{in}} - \sum_{i=1}^{6} p_i\right) \tfrac{1}{2} \sum_{s_i s_f} |M^{s_i s_f}|^2 , \tag{A1}$$

where $M^{s_i s_f}$ is the symmetrized $2 \to 6$ amplitude for initial (final) proton spin s_i (s_f). It will be written as the sum over the twelve permutations

$$M^{s_i s_f} = \sum_{j=1}^{12} M_j^{s_i s_f} . \tag{A2}$$

We define the standard permutation $j = 1$ corresponding to Fig. 16, where the momenta of $(\pi^+\pi^-)$ $(\pi^+\pi^-)$ $(\pi^+ p)$ are $(p_1 p_2)$ $(p_3 p_4)$ $(p_5 p_6)$. For this permutation

$$M_{j=1}^{s_i s_f} = M_{\pi\pi}(s_{12}, t_{12}; m_\pi^2, t_{23}) P(t_{23}) \times M_{\pi\pi}(s_{34}, t_{34}; t_{23}, t_{45}) \times P(t_{45}) M_{\pi p}^{s_i s_f}(s_{56}, t_{56}; t_{45}) . \tag{A3}$$

Here $s_{ij} = (p_i + p_j)^2$ and $t_{ij} = (q_{\text{in}} - \sum_{k=1}^{i} p_k)^2$, where q_{in} is the incoming pion momentum.
$M_{\pi\pi}(s, t; u_1, u_2)$ is the off-shell elastic $\pi^+\pi^-$ amplitude for initial particles of mass squared u_1 and u_2. The pion propagator is

$$P(t) = (t - m_\pi^2)^{-1} . \tag{A4}$$

The off-shell elastic $\pi^+ p$ amplitude $M_{\pi p}^{s_i s_f}(s, t; t_\pi)$ has the initial pion at $q_i^2 = t_\pi$ and the other particles on shell. Its spin structure is

$$M_{\pi p}^{s_i s_f}(s, t; t_\pi) = \bar{u}^{s_f}(p_6)[-A + \not{Q} B]\, u^{s_i}(p_{\text{in}}) , \tag{A5}$$

where $2Q = q_i + q_f$, q_f being the final pion momentum.

Defining α_j and β_j as equivalent inelastic invariant A and B amplitudes by multiplying them by

$M_{\pi\pi}PM_{\pi\pi}P$, we obtain the spin decomposition of Eq. (A2) as

$$M^{s_i s_f} = \sum_{j=1}^{12} \bar{u}^{s_f}(p_6)[-\alpha_j + \not{Q}_j\beta_j]\, u^{s_i}(p_{\rm in}) , \tag{A6}$$

with $Q_j = \frac{1}{2}(p_6 - p_{\rm in} + 2q_{5j})$ being the jth permutation of $\frac{1}{2}(q_i + q_f)$ in the elastic $\pi^+ p$ amplitude at the end of the chain. With the projection operator $(\not{p} + m_N)$ we obtain

$$\tfrac{1}{2}\sum_{s_i s_f}|M^{s_i s_f}|^2 = \mathrm{Re}\sum_{I,J=1}^{12}\{(m_N{}^2 + p_{\rm in}\cdot p_6)\alpha_I\alpha_J^* + [(m_N{}^2 - p_{\rm in}\cdot p_6)Q_I\cdot Q_J + (Q_I\cdot p_{\rm in})(Q_J\cdot p_6) + (Q_I\cdot p_6)(Q_J\cdot p_{\rm in})]\beta_I\beta_J^* - 2m_N Q_J\cdot(p_{\rm in}+p_6)\alpha_I\beta_J^*\} . \tag{A7}$$

The off-shell $\pi^+\pi^-$ amplitudes are parametrized by

$$M_{\pi\pi}(s,t;u_1,u_2) = \frac{16\pi s}{\lambda^{1/2}(s,m_\pi{}^2,m_\pi{}^2)}\, V_{\rm off}(u_1,u_2) \times \sum_{I,l}(2l+1)c_l^I P_l(\cos\theta_{\rm off}) \times e^{i\delta_l^I}\sin\delta_l^I , \tag{A8}$$

where $c_{2l}^0 = \frac{2}{3}$, $c_{2l}^2 = \frac{1}{3}$, and $c_{2l+1}^1 = 1$, the others being zero. $\cos\theta_{\rm off}$ is the cosine of the off-shell scattering angle, and our off-shell vertex $V_{\rm off}(u_1,u_2)$ common to all partial waves is

$$V_{\rm off}(u_1,u_2) = \left(1 - \frac{\tilde{u}_1}{\lambda} - \frac{\tilde{u}_2}{\lambda} + \frac{\tilde{u}_1\tilde{u}_2}{\xi}\right)e^{b(\tilde{u}_1+\tilde{u}_2)} , \tag{A9}$$

where $\tilde{u} = u - m_\pi{}^2$. The values of the parameters used were (see text)

$$\lambda = 1.2\ \mathrm{GeV}^2 , \quad b = 0.6\ \mathrm{GeV}^{-2} , \quad \xi = 0.15\ \mathrm{GeV}^4 . \tag{A10}$$

The calculations were performed using the on-shell s-, p-, and d-wave phase shifts[13] which were assumed elastic, and the integrals were cut off for $\pi\pi$ subenergies above 1.5 GeV. These approximations are reasonable for σ_6^+ at these energies.

We next consider the (conventional) πp parametrization. As we are neglecting exotic $\pi\pi$ channels, the only πp state required is $I = \frac{3}{2}$. Here, the only important partial waves are the $l=0$ wave s_{31} and the $l=1$ wave p_{33}. The Benecke-Dürr continuation relates the scattering in each wave to the physical amplitude.[8] The off-shell invariant amplitudes are

$$A(s,t;t_\pi) = 4\pi\left(\frac{a_+}{b_+}f_1 - \frac{a_-}{b_-}f_2\right) , \tag{A11}$$

$$B(s,t;t_\pi) = 4\pi\left(\frac{1}{b_+}f_1 + \frac{1}{b_-}f_2\right) , \tag{A12}$$

where

$$f_1 = \frac{1}{q_{\rm on}}\left[f_{\rm off}^{I=0}P_1'(\hat{z}) + f_{\rm off}^{I=1}P_2'(\hat{z})\right]\frac{q_+(t_\pi)}{q_+(m_\pi{}^2)} , \tag{A13}$$

$$f_2 = -\frac{1}{q_{\rm on}}f_{\rm off}^{I=1}P_1'(\hat{z})\,\frac{q_+(t_\pi)}{q_+(m_\pi{}^2)} . \tag{A14}$$

Here $q_{\rm on}$ ($q_{\rm off}$) is the on (off)-shell πp c.m. momentum, $\hat{z} = \cos\theta_{\rm off}(t_\pi)$,

$$a_\pm = s^{1/2} \pm m_N , \quad b_\pm = \frac{1}{2s^{1/2}}\, q_\pm(t_\pi)q_\pm(m_\pi{}^2) , \quad q_\pm(x) = [(s^{1/2}\pm m_N)^2 - x]^{1/2} , \tag{A15}$$

and

$$f_{\rm off}^I = \frac{v_I(q_{\rm off}R_I)}{v_I(q_{\rm on}R_I)}f_{\rm on}^I . \tag{A16}$$

The Benecke-Dürr functions v_I required are[4]

$$v_0(x) = \frac{1}{4x^2}\ln(1+4x^2) , \quad v_1(x) = \frac{1}{4x^2}\left[\left(1+\frac{1}{2x^2}\right)\ln(1+4x^2) - 2\right] . \tag{A17}$$

The value of R_1 (=1.76) is taken from the fits of Wolf (Ref. 4), and R_0 was set equal to zero (which is very close to Wolf's value), so that v_0 becomes simply unity.

The πN phase shifts and elasticities were taken from Ref. 14 and used up to πN subenergies of 2 GeV, above which the integration was cut off.

For computer purposes, we have employed a simplification, which we now describe. For any differential distribution $d\sigma_6^+/dv$ in the variable v, we have (omitting the spin indices but retaining permutation indices)

$$\frac{d\sigma_6^+}{dv} = \tfrac{1}{12}\int d\Phi_6(v)\sum_{I=1}^{12}\sum_{J=1}^{12} M_I M_J^* , \tag{A18}$$

where M_j is the unsymmetrized $2\to 6$ amplitude corresponding to the jth permutation of the momenta $\{p_1\cdots p_6\}$ generated by FOWL for that event.

The measure $d\Phi_6(v)$ is symmetric in the identical particle momenta (i.e., we add histograms of all identical particle combinations). Now any given integral $\int M_l M_j^*$ can always be made equal to an integral $\int M_1 M_k^*$, where $k = k(l,j)$ is some permutation which is distinct for given l,j. This follows from simply changing variables in the integral so that permutation l becomes the standard permutation 1. Hence the double sum in Eq. (A18) collapses, and we obtain

$$\frac{d\sigma_6^+}{dv} = \mathrm{Re} \int d\Phi_6(v) \sum_{k=1}^{12} M_1 M_k^* \,. \qquad \text{(A19)}$$

It should be clear that this equality holds formally, but since the computer only performs integrations approximately by random generation of points, it is actually only valid up to some statistical error in practice. Considerable computer time is saved by this trick, although due to statistical errors occasional negative weights are generated (giving, in fact, an estimate of "reasonable computer statistics"). In the limit of infinite statistics, Eq. (A19) is exact without taking the real part.

To save further computer time we have only calculated the first four terms of the sum since they account for practically all of σ_6^+ (see text).

---

*Part of this work performed under the auspices of the U. S. Atomic Energy Commission.

†Summer visitor at the University of Washington, Seattle, Wash. 98195.

‡Summer visitor at Argonne National Laboratory, Argonne, Ill. 60439.

[1]D. Amati, A. Stanghellini, and S. Fubini, Nuovo Cimento 26, 896 (1962); L. Bertocchi, S. Fubini, and M. Tonin, *ibid.* 25, 626 (1962).

[2]G. F. Chew, T. Rogers, and D. R. Snider, Phys. Rev. D 2, 765 (1970).

[3]J. Dash, G. Parry, and M. Grisaru, Nucl. Phys. B53, 91 (1973).

[4]Gunter Wolf, Phys. Rev. 182, 1538 (1969).

[5]A. Jurewicz, L. Michejda, J. Namyslowski, and J. Turnau, Nucl. Phys. B29, 269 (1971); J. Huskins, thesis, 1973 (unpublished).

[6]G. F. Chew and D. Snider, Phys. Rev. D 1, 3453 (1970); *ibid.* 3, 420 (1971); J. Dash, Phys. Rev. D 9, 200 (1974).

[7]W. Kittel, Report No. CERN 73-10, 1973 (unpublished). One of us (J.H.) has also found the threshold behavior of the ABFST model to be too small in the case $p\bar{p} \to p\bar{p}2\pi^+2\pi^-$ for $p_{\mathrm{lab}} < 7$ GeV/c. No higher-energy data are available to enable a real test of the model in this case.

[8]In Ref. 3, the two parameters b and ξ in the $\pi\pi$ off-shell vertex V_{off} are not used. However, V_{off} is numerically similar to the off-shell prescription used there. The parameter ξ is needed for getting detailed agreement with experiment. Setting $\xi = \infty$ and adjusting b to a smaller value still yields qualitatively correct results.

[9]J. Benecke and H. P. Dürr, Nuovo Cimento 56, 269 (1968).

[10]H. Drevermann *et al.*, Phys. Rev. 161, 1356 (1967).

[11a]ABB-CERN-CDDHNP (EP)-STW Collaboration, CERN Report No. 72-32, 1972 (unpublished).

[11b]ABB-CERN-CDDHNP (EP)-STW Collaboration, CERN Report No. 72-37, 1972 (unpublished).

[12]F. James, Institute de Physique Nucléaire (Paris) report, 1966 (unpublished). Users of this program should be aware that the random number generator must be put in double precision on certain computers with less than CDC accuracy.

[13]J. F. C. Hopkinson and R. G. Roberts, Nuovo Cimento 59, 181 (1969).

[14]D. J. Herndon, A. Barbaro-Galtieri, and A. H. Rosenfeld, Report No. UCRL-20030πN, 1970 (unpublished).